Developmental Cell
Short Article

Ectodermal Smad4 and p38 MAPK Are Functionally Redundant in Mediating TGF-β/BMP Signaling during Tooth and Palate Development

Xun Xu,[1] Jun Han,[1] Yoshihiro Ito,[1] Pablo Bringas, Jr.,[1] Chuxia Deng,[2] and Yang Chai[1,*]
[1]Center for Craniofacial Molecular Biology, University of Southern California, 2250 Alcazar Street, CSA 103, Los Angeles, CA 90033, USA
[2]Genetics of Development and Disease Branch, NIDDK, NIH, Building 10, Bethesda, MD 20892, USA
*Correspondence: ychai@usc.edu
DOI 10.1016/j.devcel.2008.06.004

SUMMARY

Smad4 is a central intracellular effector of TGF-β signaling. Smad-independent TGF-β pathways, such as those mediated by p38 MAPK, have been identified in cell culture systems, but their in vivo functional mechanisms remain unclear. In this study, we investigated the role of TGF-β signaling in tooth and palate development and noted that conditional inactivation of Smad4 in oral epithelium results in much milder phenotypes than those seen with the corresponding receptor mutants, *Bmpr1a* and *Tgfbr2*, respectively. Perturbed p38 function in these tissues likewise has no effect by itself; however, when both Smad4 and p38 functions are compromised, dramatic recapitulation of the receptor mutant phenotypes results. Thus, our study demonstrates that p38 and Smad4 are functionally redundant in mediating TGF-β signaling in diverse contexts during embryonic organogenesis. The ability of epithelium to utilize both pathways illustrates the complicated nature of TGF-β signaling mechanisms in development and disease.

INTRODUCTION

TGF-β/BMP signaling plays an important role in pattern formation and organogenesis (Andl et al., 2004; Chai and Maxson, 2006; Xu et al., 2006). In the craniofacial region, BMP is a critical regulator of the epithelial-mesenchymal interaction during tooth development. Epithelial BMP4 induces the expression of *Msx1* in the dental mesenchyme, then *Msx1* further induces *Bmp4* expression in the mesenchyme. Ectopic BMP4 can rescue the defective tooth phenotype in *Msx1*-deficient mice (Zhao et al., 2000). BMP4 also induces the expression of *p21* and *Msx2* in the dental epithelium and is associated with enamel-knot formation (Jernvall et al., 1998). Ablation of *Bmpr1a* in the dental epithelium causes the arrest of tooth development at the early bud stage (Andl et al., 2004; Liu et al., 2005).

TGF-β signaling also plays an important role in regulating palatogenesis. During mouse palate development, TGF-β1 and TGF-β3 are expressed in the medial edge epithelium (MEE), whereas TGF-β2 is expressed in the mesenchyme beneath the MEE (Fitzpatrick et al., 1990; Pelton et al., 1990). *Tgfb3*-null mutant mice exhibit cleft palates, with 100% phenotype penetrance (Kaartinen et al., 1995; Proetzel et al., 1995), and the failure of palatal fusion can be rescued by adding exogenous TGF-β3 in an organ culture model (Brunet et al., 1995; Taya et al., 1999). TGF-β3 is required for the fusion of palatal shelves by inducing apoptosis in the MEE (Martinez-Alvarez et al., 2000). TGF-β IIR is expressed in both the MEE and the cranial neural crest (CNC)-derived palatal mesenchyme (Cui et al., 1998). Ablation of *Tgfbr2* in the palatal mesenchyme compromises cell proliferation and causes complete cleft palate (Ito et al., 2003), whereas ablation of *Tgfbr2* in the palatal epithelial cells suppresses apoptosis and results in both soft palate cleft and submucosal cleft (Xu et al., 2006).

The canonical TGF-β/BMP signaling pathway includes binding of the ligand to initiate the assembly of a heteromeric complex of type II and type I receptors. The activated type I receptor phosphorylates the receptor-regulated Smads (R-Smad), which bind to common Smad (Smad4) and move into the nucleus. In the nucleus, this Smad complex associates with other transcription factors to regulate the expression of target genes. Although Smad4 occupies the central part of this signaling cascade (Massague, 1998; Pelton et al., 1990), studies with Smad4-deficient cells, or dominant-negative Smads, support the possibility that TGF-β/BMP signaling can operate in a Smad4-independent manner (Derynck and Zhang, 2003). TGF-β can activate mitogen-activated protein kinases (MAPK) signaling pathways, which include extracellular signal-regulated kinase (Erk), c-Jun N-terminal kinases (JNKs), and p38 kinases pathways (Adachi-Yamada et al., 1999; Hartsough and Mulder, 1995; Yu et al., 2002). However, the in vivo mechanism for this Smad4-independent TGF-β/BMP signaling pathway and the role of Smad4 in craniofacial development still remain unclear.

In this study, we inactivated the *Smad4* gene in both dental and palatal epithelium, and we show that Smad4 is required for the proper patterning of dental cusps. However, ablation of *Smad4* in dental and palatal epithelium does not block early tooth development or palatal fusion. The p38 MAPK is activated by TGF-β and can function as a complementary effector to mediate Smad4-independent TGF-β signaling during tooth and palate development.

RESULTS

Cre-Mediated Inactivation of Smad4 in the Dental Epithelium Causes Dental Cusp Patterning Defects

Loss of *Smad4* leads to early embryonic mortality by embryonic day 7 (E7). To bypass this early embryonic lethality and study the

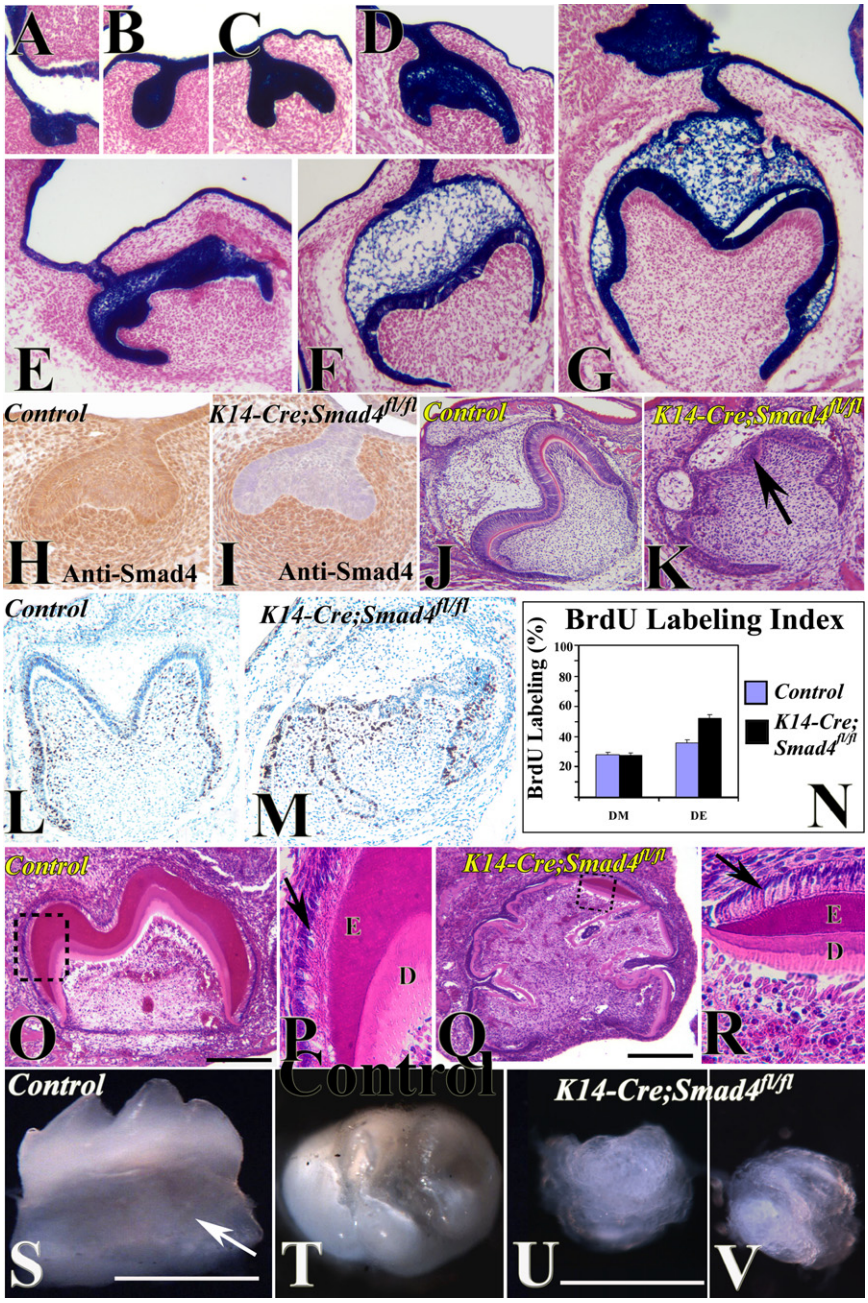

Figure 1. Severe Tooth Defects in *K14-Cre;Smad4$^{fl/fl}$* Mice

(A–G) X-gal staining of *K14-Cre;R26* mice. (A) E12.5, lamina stage. (B) E13.5, bud stage. (C) E14.5, cap stage. (D) E15.5, stage 23. (E) E16.5, bell stage. (F) E17.5, stage 25. (G) Newborn.

(H and I) Smad4 (red staining) in the (H) control and (I) *K14-Cre;Smad4$^{fl/fl}$* tooth germ.

(J and K) Hematoxylin and eosin staining of molar tooth germ from (J) control and (K) *K14-Cre;Smad4$^{fl/fl}$* newborn mice. The arrow indicates the disorganized cell mass located in the dental epithelium.

(L–N) BrdU assay in E17.5 (L) control and (M) *K14-Cre;Smad4$^{fl/fl}$* tooth germ. (N) BrdU labeling index of control and mutant tooth germ. DM, dental mesenchyme; DE, dental epithelia. The error bars indicate 95% confidence intervals. *$p < 0.05$.

(O–R) Tooth germ from (O and P) control samples and (Q and R) *K14-Cre;Smad4$^{fl/fl}$* mice cultured under kidney capsule for 14 days. (P) and (R) are enlarged views of the dotted boxes in (O) and (Q), respectively. Arrows in (P) and ® indicate ameloblast cells. D, dentin; E, enamel. The scale bar represents 200 μm.

(S–V) Tooth germ from (S and T) control and (U and V) *K14-Cre;Smad4$^{fl/fl}$* mice cultured 28 days under kidney capsule, (S) and (U) show buccal views, and (T) and (V) show occlusal views. The arrow in (S) indicates the root. The scale bar represents 1 mm.

role of Smad4 during tooth development, we crossed a *Smad4* conditional allele (Yang et al., 2002) with *K14-Cre* transgenic mice (Andl et al., 2004) to generate *K14-Cre;Smad4$^{fl/fl}$* mutant embryos. At birth, we recovered *K14-Cre;Smad4$^{fl/fl}$* pups at the expected Mendelian frequency. The *K14-Cre;Smad4$^{fl/fl}$* mice died soon after birth and lacked milk in their stomachs.

The *K14-Cre* transgene directed Cre activity in the dental epithelium in *K14-Cre;R26R* samples (Figures 1A–1G). At E12.5, the lamina stage of tooth development, Cre recombinase is robustly expressed in every cell in the dental epithelium, as demonstrated by *lacZ* staining (Figure 1A). This expression pattern of Cre recombinase was consistent throughout all stages of tooth development until birth. Examination of serial sections from E12.5 to newborn mice did not reveal any β-galactosidase-positive cells in the dental mesenchyme (Figures 1A–1G and data not shown), suggesting that this *K14-Cre* line can effectively and precisely mediate gene inactivation in the dental epithelium. The successful inactivation of Smad4 was confirmed by immunohistochemical staining by using an antibody to Smad4. We found that the dental epithelial cells in *K14-Cre;Smad4$^{fl/fl}$* tooth germ were negative for Smad4 (Figures 1H and 1I).

Surprisingly, tooth development progressed beyond the cap stage without obvious defects in *K14-Cre;Smad4$^{fl/fl}$* mice. In contrast, tooth development arrested at the early bud stage in *Bmpr1a*-deficient mice (Andl et al., 2004; Liu et al., 2005). At the newborn stage, the dental epithelium of *K14-Cre;Smad4$^{fl/fl}$* mice exhibited severe defects: the differentiation of the inner enamel epithelium was delayed, no clear dental cusps were present, and there was a disorganized cell mass located in the dental epithelium (Figures 1J and 1K). We hypothesized that altered dental epithelial cell proliferation or apoptosis activity might have contributed to the disorganization of dental cusp patterning. BrdU incorporation analysis indicated that the *Smad4* mice exhibited a significant increase ($p < 0.05$) in cell proliferation in the dental epithelium (Figures 1L–1N). Because the *Smad4* mice could not survive after birth, we cultured the tooth germ

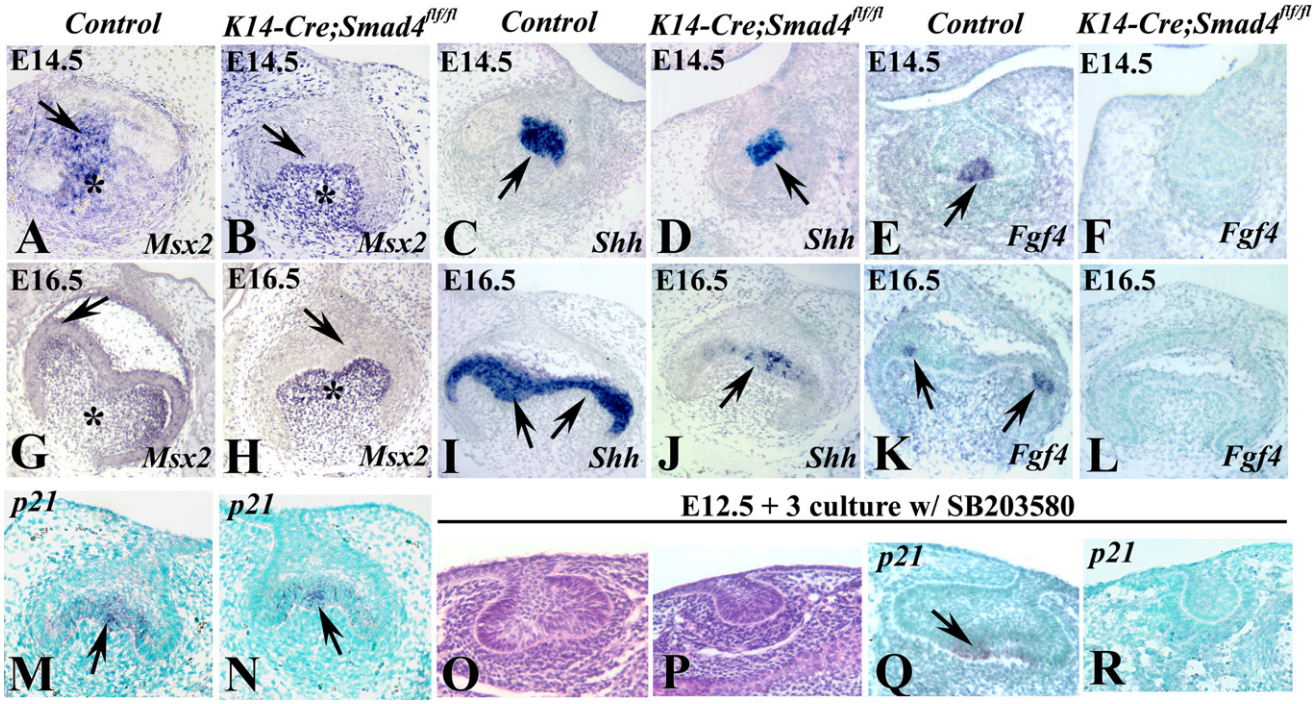

Figure 2. Dental Cusp Patterning Gene Expression Analyses by In Situ Hybridization

(A–L) (A and G) *Msx2* is expressed in the dental epithelium (arrow) and dental mesenchyme (*) in control tooth germ. (B and H) *Msx2* expression is undetectable in *K14-Cre;Smad4*$^{fl/fl}$ dental epithelium. (C and D) Expression of *Shh* in control and *K14-Cre;Smad4*$^{fl/fl}$ tooth germ is comparable at E14.5. (I and J) *Shh* expression is significantly reduced in *K14-Cre;Smad4*$^{fl/fl}$ tooth germ at E16.5. (E and K) *Fgf4* is expressed in both primary and secondary enamel knots in control tooth germ. (F and L) *Fgf4* is not detectable in the *K14-Cre;Smad4*$^{fl/fl}$ tooth germ.

(M and N) *p21* is expressed in the primary enamel knot of both control and *K14-Cre;Smad4*$^{fl/fl}$ tooth germ (arrow).

(O–R) Mandibular organ culture with the p38 inhibitor SB203580. In the control sample, (O) tooth germ successfully developed to the cap stage after 3 days, and (Q) the primary enamel knot formed, as assayed by *p21* expression (arrow). (P and R) The *K14-Cre;Smad4*$^{fl/fl}$ tooth germ is arrested at the bud stage, and there is no *p21* expression.

by using kidney capsule grafting in order to investigate the biological function of Smad4 signaling in regulating postnatal tooth development. After 2 weeks of culture, some mutant dental epithelial cells differentiated into ameloblasts and formed enamel matrix, which suggests that Smad4 is dispensable for ameloblast differentiation (Figures 1Q and 1R). However, the Smad4 mutant tooth germ showed severe defects in the patterning of the dental cusps (Figures 1Q and 1R), compared with the control samples (Figures 1O and 1P). After 4 weeks of culture, control tooth germ developed into a well-formed tooth (Figures 1S and 1T). In contrast, *Smad4* mutant tooth germ failed to form dental cusps (Figures 1U and 1V); only a fragment of tooth-like structure can be identified.

Defective Patterning of the Dental Epithelium in *K14-Cre;Smad4*$^{fl/fl}$ Tooth Germ

To investigate the patterning defects in the *K14-Cre;Smad4*$^{fl/fl}$ dental cusps, we performed gene marker analyses in control and *K14-Cre;Smad4*$^{fl/fl}$ molar tooth germ. *Msx2* and *Shh*, downstream targets of BMP signaling, were downregulated in *K14-Cre;Smad4*$^{fl/fl}$ tooth germ. In the control tooth germ, *Msx2* was expressed in both dental epithelium and mesenchyme (Figures 2A and 2G). *Msx2* expression was completely absent in the *K14-Cre;Smad4*$^{fl/fl}$ mutant dental epithelium, whereas the expression level in the dental mesenchyme remained comparable to that in the control tooth germ (Figures 2B and 2H). *Shh* was expressed in the primary enamel knot during the cap stage in control tooth germ (Figure 2C). As tooth development progressed, *Shh* expression extended into the entire inner enamel epithelium and stratum intermedium (Figure 2I). In the *K14-Cre;Smad4*$^{fl/fl}$ mutant tooth germ, *Shh* expression was fairly comparable to what was seen in control sample at E14.5 (Figure 2D), but it failed to extend in the later stage (Figure 2J). *Fgf4*, which is specifically expressed in enamel knots, was not expressed in the *K14-Cre;Smad4*$^{fl/fl}$ tooth germ, indicating that enamel-knot formation was deficient in *Smad4* mutant tooth germ (Figures 2E, 2F, 2K, and 2L).

Smad4 and p38 MAPK Function Redundantly to Regulate Early Tooth Development

The development of tooth germ in *K14-Cre;Smad4*$^{fl/fl}$ mice was fairly comparable morphologically to that of control sample at E14.5. Moreover, we detected *p21* expression in the enamel-knot area (Figures 2M and 2N). Previous studies have indicated that members of the TGF-β superfamily can activate Smad4-independent signaling cascades, such as MAPK pathways (Derynck and Zhang, 2003; Yu et al., 2002). Although there are three subgroups of the MAPK superfamily (JNK, p38, Erk MAPK), p38 MAPK is the only one that has been implicated to date in TGF-β-superfamily signal transduction in *Drosophila* wing

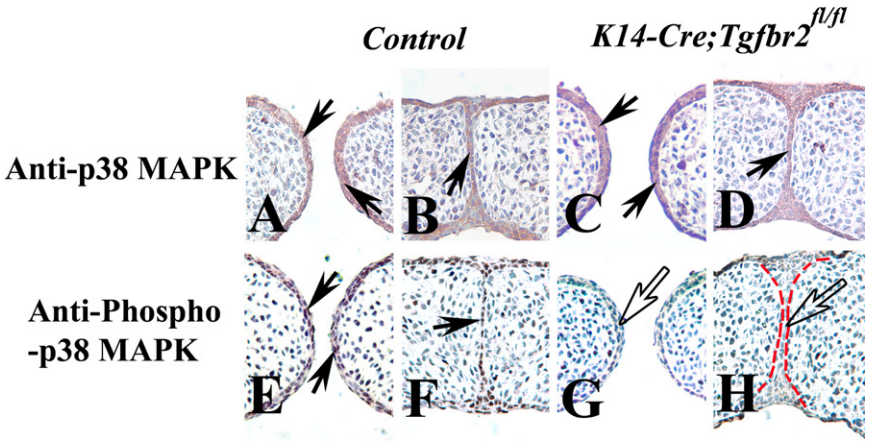

Figure 3. TGF-β Is Required for the Activation of p38 MAPK in the Palatal Epithelium

(A– H) (A–D) By immunohistochemistry, p38 MAPK is detected in both (A and B) control and (C and D) *K14-Cre;Tgfbr2*$^{fl/fl}$ mutant palatal epithelium. (E–H) Phospho-p38 MAPK can only be detected in the (E and F) control palatal epithelium, but not in the (G and H) *K14-Cre;Tgfbr2*$^{fl/fl}$ mutant palatal epithelium. Arrows indicate positive signals in the palatal epithelium. The open arrows in (G) and (H) indicate epithelial cells that were negative for phospho-p38 MAPK. The red, broken line indicates the persistent MEE cells.

morphogenesis (Adachi-Yamada et al., 1999). We hypothesized that a similar signaling scenario might be operative in regulating mammalian organogenesis. To test whether p38 MAPK can mediate Smad4-independent BMP signaling in tooth development, we blocked p38 activity by using the imidazole compound SB203580, a p38 MAPK-specific inhibitor, in our mandibular organ culture model. Control tooth germ from E12.5 embryos developed from the bud to the cap stage, as validated by positive *p21* expression after 3 days of culture in the presence of the p38 MAPK inhibitor (n = 20) (Figures 2O and 2P). In contrast, the development of *K14-Cre;Smad4*$^{fl/fl}$ tooth germ was arrested at the bud stage after the addition of SB203580, as judged by the lack of *p21* expression in the enamel epithelium (Figures 2Q and 2R). The same effect was seen in all 12 *K14-Cre;Smad4*$^{fl/fl}$ mandible explants. To rule out the possibility that the arrested tooth phenotype in *K14-Cre;Smad4*$^{fl/fl}$ tooth germ was due to delayed development, we also extended the culture time to 5 days; the *K14-Cre;Smad4*$^{fl/fl}$ tooth germ treated with SB203580 was still arrested at the bud stage (data not shown).

Smad4 Is Dispensable for Palatal Fusion in the Epithelium

Loss of *Tgfb3* or tissue-specific inactivation of *Tgfbr2* or *Tgfbr1* in the palatal epithelium results in cleft palate with complete phenotype penetrance (Xu et al., 2006; Dudas et al., 2006; Kaartinen et al., 1995). Interestingly, however, palatal epithelial tissue-specific inactivation of *Smad4* did not adversely affect palatal fusion. At birth, the palate formed normally in *K14-Cre;Smad4*$^{fl/fl}$ mutant mice (Figures S1A and S1B, available online). Histological analysis revealed confluent palatal mesenchyme without any residue of epithelial cells at the midline in both control and *K14-Cre;Smad4*$^{fl/fl}$ mice (Figures S1C and S1D). Moreover, we confirmed that we had specifically and completely eliminated Smad4 from the palatal epithelium prior to palatal fusion, as judged by immunohistochemical analysis (Figures S1E and S1F). These data strongly suggest that a Smad4-independent pathway is also involved in regulating palatogenesis.

Smad4 and p38 MAPK Function Redundantly to Regulate TGF-β-Induced Palatal Fusion

Prior to palatal fusion, p38 MAPK was mainly expressed in palatal epithelial cells, whereas there was only sporadic expression in the palatal mesenchyme (Figures 3A and 3B). When we blocked TGF-β signaling in *K14-Cre;Tgfbr2*$^{fl/fl}$ mice, p38 MAPK expression was not affected in the developing palate, implying that the expression of p38 MAPK is not dependent upon TGF-β signaling (Figures 3C and 3D). Significantly, p38 MAPK was activated in the palatal epithelium prior to palatal fusion, as indicated by anti-phospho-p38 MAPK staining (Figures 3E and 3F). In the absence of TGF-β signaling, however, we failed to detect the activation of p38 MAPK in the palatal epithelium of *K14-Cre;Tgfbr2*$^{fl/fl}$ mice (Figures 3G and 3H), suggesting that TGF-β signaling is required for the activation of p38 MAPK activity in the palatal epithelium.

To test whether p38 MAPK is required as a Smad4-independent TGF-β signaling effector during palatal fusion, we conducted experiments with the palatal organ culture model with either siRNA or SB203580 to inactivate p38 MAPK activity. Our control experiment showed that siRNA can effectively enter the palatal epithelium prior to fusion (Figure 4G), and that siRNA treatment alone will not interfere with the palatal fusion process in vitro (Figure S2). The treatment of palatal explants with p38 MAPK siRNA significantly reduced the expression level of p38 MAPK in the palatal explants (Figures 4H and 4I). Blocking p38 MAPK activity in control samples with the addition of siRNA did not affect palatal fusion (n = 13) (Figures 4A and 4D). In contrast, inactivation of p38 MAPK in *K14-Cre;Smad4*$^{fl/fl}$ samples resulted in the failure of palatal fusion and the persistence of midline epithelial cells (n = 7) (Figures 4B and 4E), a phenotype identical to the palatal fusion failure seen in *K14-Cre;Tgfbr2*$^{fl/fl}$ samples (Figures 4C and 4F).

In parallel, inactivation of p38 MAPK in control samples with the addition of SB203580 did not affect palatal fusion in vitro (n = 14) (Figures 4J and 4M). When we added SB203580 to *K14-Cre;Smad4*$^{fl/fl}$ samples in culture, palatal fusion was retarded and midline epithelial cells persisted (n = 18) (Figures 4K, 4L, 4N, and 4O). This phenotype is indistinguishable from that of the *K14-Cre;Tgfbr2*$^{fl/fl}$ mutant sample (Figures 4C and 4F). To further clarify whether p38 MAPK functions downstream of TGF-β signaling, we cultured *Tgfb3*$^{-/-}$*;K14-Cre;Smad4*$^{fl/fl}$ compound mutant palatal shelves. Exogenous TGF-β3 is still able to rescue the palatal fusion in these compound mutant samples (n = 2) (Figures 4R and 4U), implying that TGF-β signaling can still be transmitted successfully in the absence of Smad4. However, in

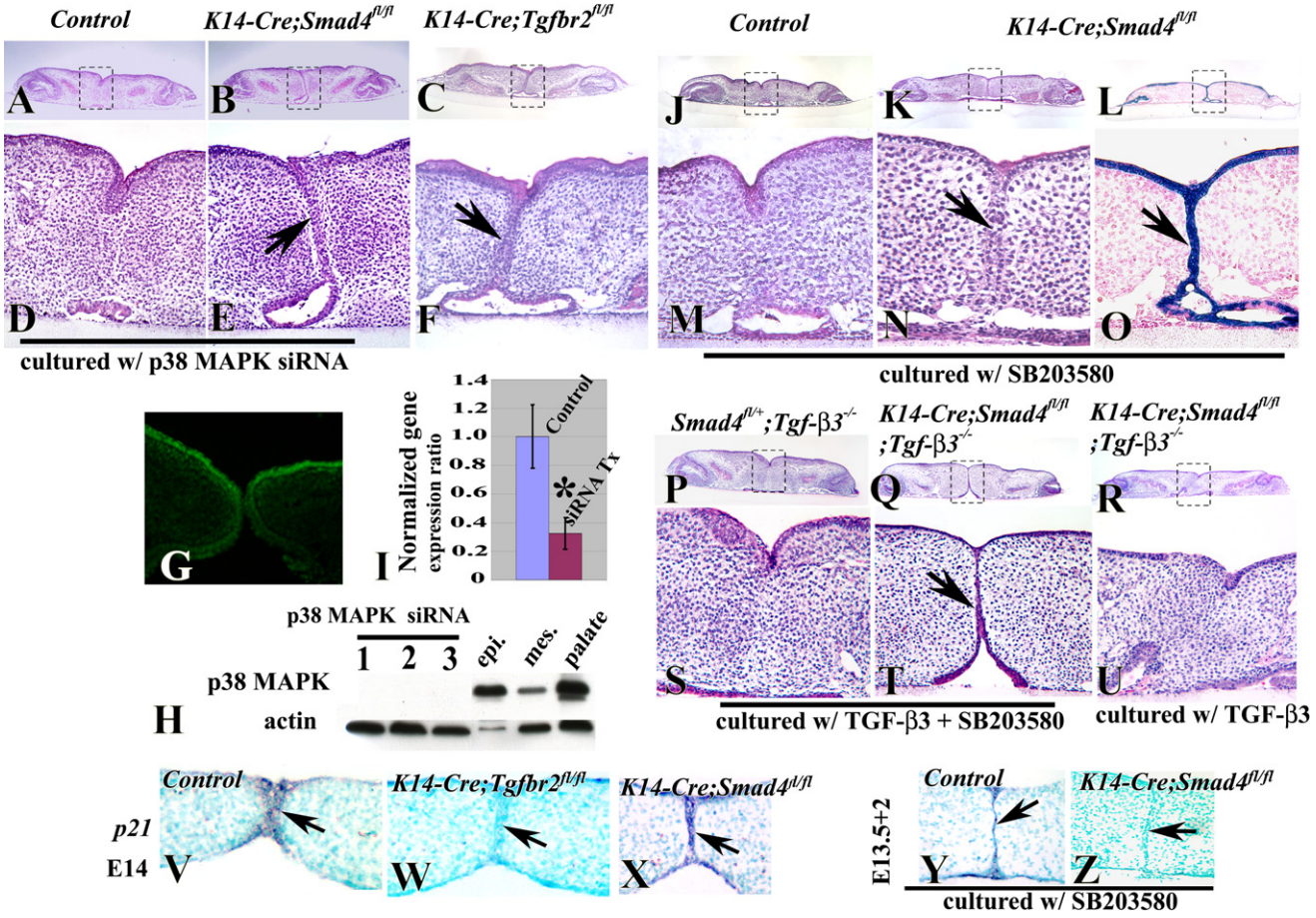

Figure 4. Smad4 and p38 MAPK Are Functionally Redundant in Mediating TGF-β Signaling during Palatal Fusion

(A–Z) Haematoxylin and eosin staining shows (A and D) control palatal shelves treated with p38 MAPK siRNA fused after 3 days culture. The boxed area in (A) is enlarged and shown as (D). (B and E) *K14-Cre;Smad4*$^{fl/fl}$ mutant palatal shelves treated with p38 MAPK siRNA show persistence of MEE cells in the palate after 3 days of culture. (C and F) Palatal culture (without inhibitor in the medium) of *K14-Cre;Tgfbr2*$^{fl/fl}$ shows the persistence of MEE cells. (G) Fluorescent detection of control siRNA in palatal epithelium (green fluorescent protein). (H) Western blot analysis shows that p38 MAPK is knocked down by siRNA in the palatal culture system (lanes 1–3, protein extracted from siRNA-treated samples [experiments were repeated three times]). Epi, palatal epithelium; mes, palatal mesenchyme; palate, whole palate. (I) The p38 MAPK expression level is significantly knocked down by siRNA treatment (the error bar indicates a 95% confidence interval; *$p < 0.01$). The values were expressed relative to that of control. (J and M) After 3 days of culture with SB203580, control E13.5 palatal shelves fused. (K, L, N, and O) *K14-Cre;Smad4*$^{fl/fl}$ mutant palatal shelves show the persistence of MEE cells (arrow) after 3 days of culture with SB203580. (L and O) lacZ staining. (P and S) Exogenous TGF-β3 can rescue *Tgfb3*$^{-/-}$;*Smad4*$^{fl/+}$ palatal fusion in medium containing SB203580. (Q and T) Exogenous TGF-β3 fails to rescue *Tgfb3*$^{-/-}$;*K14-Cre;Smad4*$^{fl/fl}$ palatal fusion in medium containing SB203580. (R and U) Exogenous TGF-β3 can rescue *Tgfb3*$^{-/-}$;*K14-Cre;Smad4*$^{fl/fl}$ palatal fusion. (V–Z) In situ hybridization of *p21* in palatal shelves of (V) control, (W) *K14-Cre;Tgfbr2*$^{fl/fl}$, and (X) *K14-Cre;Smad4*$^{fl/fl}$ mice, untreated or cultured with SB203580; (Y) control sample; (Z) *K14-Cre;Smad4*$^{fl/fl}$ sample. Dark blue indicates *p21* expression. The arrow indicates MEE cells.

the presence of SB203580, exogenous TGF-β3 failed to rescue palatal fusion in *Tgfb3*$^{-/-}$;*K14-Cre;Smad4*$^{fl/fl}$ samples (n = 3) (Figures 4Q and 4T). On the other hand, inhibition of p38 MAPK did not prevent exogenous TGF-β3 from restoring palatal fusion in *Tgfb3*$^{-/-}$ mutant palatal shelves (n = 5) (Figures 4P and 4S).

Apoptosis is a major fate of palatal shelf midline epithelial cells in which *p21* is expressed prior to palatal fusion (Figure 4V). In *K14-Cre;Tgfbr2*$^{fl/fl}$ mice, we detected diminished apoptosis in the epithelium prior to fusion and persistence of the epithelial seam, but we failed to detect *p21* expression (Figure 4W). These data suggest that TGF-β signaling is required for *p21* expression in order to induce apoptosis in epithelial cells. Interestingly, neither tissue-specific inactivation of *Smad4* in the palatal epithelium nor blocking p38 MAPK by SB203580 affects *p21* expression (Figures 4X and 4Y). We were only able to prevent *p21* expression when we blocked p38 MAPK activity in the *K14-Cre;Smad4*$^{fl/fl}$ sample (n = 8), a combination that led to the persistence of midline epithelium (Figure 4Z). These data demonstrate that Smad4-dependent and -independent pathways are critical and functionally redundant in mediating TGF-β-induced *p21* expression and apoptotic activity in palatal epithelial cells prior to palatal fusion.

DISCUSSION

Smad4 is crucial for dental epithelium patterning. Disrupting the BMP signaling pathway by eliminating Smad4 in the dental

epithelium results in downregulation of *Msx2* and *Shh*, which are downstream targets of BMP signaling and are essential for the patterning of dental cusps (Bei et al., 2004; Dassule et al., 2000). However, eliminating *Smad4* alone is not sufficient to block BMP signaling in the dental epithelium during early tooth development, since it does not recapitulate the *Bmpr1a* inactivation mutation phenotype. In this study, we show that p38 MAPK functions redundantly with Smad4 to mediate BMP signaling during tooth development, and that tooth development can only be arrested at the bud stage by blocking both Smad4 and p38 MAPK. This functional redundancy is in sharp contrast to the result of loss of *Smad4* in the CNC-derived dental mesenchyme, in which tooth development is retarded at the dental laminar stage (prior to the bud stage). Thus, there is an absolute requirement for Smad4 in the CNC-derived dental mesenchyme. In addition, Smad4-mediated TGF-β/BMP signaling is required for the homeobox gene patterning of oral/aboral and proximal/distal domains within the first branchial arch (Ko et al., 2007). Therefore, in the CNC-derived mesenchyme, TGF-β/BMP signals rely on Smad4-dependent pathways to mediate epithelial-mesenchymal interactions that control craniofacial organogenesis. Previous studies have shown that BMP4 signaling is critical for mediating cell death in the enamel knot, whereas Msx1-mediated BMP signaling is critical for cell proliferation in the dental mesenchyme (Chai and Maxson, 2006; Thesleff and Sharpe, 1997). Taken together, the temporal and tissue-specific activation of Smad4-dependent or -independent BMP signaling pathways may regulate different downstream target genes and contribute to the diverse functional outcomes of BMP signaling in regulating the fate of dental epithelial and CNC-derived mesenchymal cells during tooth development.

p21, a cyclin-dependent kinase inhibitor that inhibits cell proliferation at the G1/S transition, is a well-documented downstream target gene for TGF-β/BMP signaling (Hu et al., 1999). It is considered a differentiation marker for the cells of the primary enamel knot during tooth development (Jernvall et al., 1998). It is also expressed exclusively in the MEE cells within the palatal shelf during palatogenesis. Our study shows that inactivation of *Tgfbr2* in the MEE cells leads to downregulation of *p21* and failure of palatal fusion. These results further confirm that *p21* works downstream of TGF-β signaling during palatogenesis. However, in the absence of *Smad4*, the expression of *p21* is unchanged and palatal shelves can fuse without any obvious defects. After blocking p38 MAPK, *p21* expression is reduced and palatal fusion is compromised in the *K14-Cre;Smad4$^{fl/fl}$* mice. Clearly, *p21* expression and palatal fusion are controlled by two parallel signals: Smad4 and p38 MAPK. The results of culture experiments with *Tgfb3$^{-/-}$;K14-Cre;Smad4$^{fl/fl}$* compound mutant palatal shelves suggest that p38 MAPK is activated by TGF-β and is required specifically for transducing TGF-β signaling. Equally important, our study shows that p38 MAPK is specifically expressed in the palatal epithelium. TGF-β signaling is required for the activation of p38 MAPK, whereas it is not required for p38 expression. We have provided multiple lines of evidence that only simultaneous inactivation of Smad4 and p38 MAPK can completely block TGF-β signaling in the palatal epithelium. Thus, we conclude that Smad4-dependent and -independent pathways are critical and functionally redundant in mediating TGF-β-induced p21 activity in palatal epithelial cells.

The discovery of Smad4-dependent and -independent TGF-β/BMP signaling in the regulation of tooth and palate development has broad implications. The functional redundancy of Smad4-dependent and -independent TGF-β/BMP signaling may be used as a general mechanism in regulating organogenesis and parallels recent findings regarding the mechanism of TGF-β signaling in cancer cell development. For example, Smad4-dependent and -independent TGF-β signaling play an important role in the fate determination of mouse mammary gland epithelial cells and other tumor cells (Derynck and Zhang, 2003; Yu et al., 2002). Studies with overexpression of dominant-negative components of the Rho pathways or pharmacologic inhibitors of p38MAPK suggest that TGF-β signaling can be mediated through the Smad4-independent pathway to control the fate of tumor cells in the proinvasive and metastatic states (Bhowmick et al., 2001; Dumont and Arteaga, 2003; Tian et al., 2004). Collectively, these studies highlight the ability of the ectoderm to use Smad4 and p38 MAPK as redundant effectors for TGF-β/BMP signaling and underscore the involvement of diversified Smad4-dependent and -independent TGF-β signaling networks in regulating development and disease.

EXPERIMENTAL PROCEDURES

Generation and Analysis of Transgenic Mice

Male mice carrying the *K14-Cre* allele (Andl et al., 2004) were crossed with females carrying the *R26R* conditional reporter allele (Soriano, 1999) to generate *K14-Cre;R26R* embryos. *K14-Cre* mice were also crossed with *Smad4$^{fl/fl}$* females (Yang et al., 2002) to generate *K14-Cre;Smad4$^{fl/+}$* mice. The male *K14-Cre;Smad4$^{fl/+}$* mice were mated with *Smad4$^{fl/fl}$* female mice to generate *K14-Cre;Smad4$^{fl/fl}$* null alleles. *K14-Cre;Tgfbr2$^{fl/fl}$* mice were generated as previously described (Xu et al., 2006). The male *K14-Cre;Smad4$^{fl/+}$* mice were also mated with *Tgfb3$^{+/-}$* female mice (Proetzel et al., 1995) to generate *Tgfb3$^{+/-}$;K14-Cre;Smad4$^{fl/+}$* mice and *Tgfb3$^{+/-}$;Smad4$^{fl/+}$* mice. *Tgfb3$^{-/-}$;K14-Cre;Smad4$^{fl/fl}$* embryos were produced by crossing *Tgfb3$^{+/-}$;K14-Cre;Smad4$^{fl/+}$* and *Tgfb3$^{+/-}$;Smad4$^{fl/+}$* mice. Detection of β-galactosidase activity in tissue sections, cell proliferation, immunohistochemistry, and histological analyses were carried out as previously described (Chai et al., 2000; Xu et al., 2006). The specific anti-Smad4 antibody was purchased from Santa Cruz (cat# sc-7966), and anti-p38 MAPK and anti-phospho-p38 MAPK antibodies were purchased from Cell Signaling (cat# 9212 and 4631, respectively).

Organ Cultures and Kidney Capsule Grafting

Timed-pregnant mice were sacrificed on postcoital day 11.5 (for mandible culture) or 13.5 (for palatal culture). Genotyping was carried out as previously described. The mandibles or palatal shelves were microdissected and cultured in serum-less, chemically defined medium. SB203580 (Sigma) was added into the medium for the experimental groups at a final concentration of 15 μM. For TGF-β3, the final concentration was 10 ng/ml (R&D systems). Tissues were harvested after 3 days of culture for further processing. Kidney capsule grafting was carried out as previously described (Xu et al., 2005).

siRNA Transfection in Palatal Culture System

E13.5 palatal shelves were cultured in serum and antibiotic-free medium for 4 hr as previously described. The medium was then replaced with siRNA-containing medium. siRNA-containing medium was prepared under the following procedures (modified from the manufacture's protocol): a total of 200 μl serum-free medium was added to a clean, sterile microfuge tube; then, 4 μl Transfection Reagent (*Trans*It-TKO, Mirus) was added to the tube, and the solution was mixed by pipetting up and down; the solution was then incubated at room temperature for 5 min. A total of 12 μl stock p38 MAPK siRNA (Cell Signaling, cat# 6386 or 6385 for kit) was added to the microfuge tube, and the solution was mixed by pipetting up and down gently. The solution was incubated for 5 min at room temperature. A total of 1000 μl serum-free medium was

added to yield a final concentration of 100 nM. Cultured palatal tissues were harvested after 48 hr for western blot or real-time PCR procedures, or tissues were collected after 72 hr for histological analyses.

Quantitative PCR Analysis

Total RNA from the cultured palatal shelves was extracted by using an RNeasy mini kit and was treated with RNase-free DNase I (QIAGEN) by following the manufacturer's protocol. Superscript III with an oligo(dT)$_{20}$ primer (Invitrogen) was used for the first-strand synthesis. We carried out real-time RT-PCR on the iCycler (Bio-Rad; Hercules, CA) with gene-specific primers and with SYBR Green. All reactions were performed under the following cycling protocol: 3 min heat start at 95°C and 40 cycles of denaturation at 95°C for 1 min, annealing and extension at 60°C for 1 min. We normalized relative expression ratios to β-actin. Primer sequences for p38 MAPK (5′-TGACCCTTATGAC CAGTCCTTT-3′ and 5′-GTCAGGCTCTTCCACTCATCTAT-3′) were obtained from the Primer Bank (http://pga.mgh.harvard.edu/primerbank/index.html).

Western Analysis

Palatal shelf explants were collected after 48 hr of culture with p38 MAPK siRNA. Palatal shelves were also collected from E13.5 embryos. Ten pairs of palatal shelves from E13.5 embryos were treated with Dispase I (Roch Diagnostics cat# 04942086) on ice with a final concentration of 2 U/ml for 1 hr, then palatal epithelium was separated from mesenchyme and pooled together for protein extraction. Protein samples were loaded in each well of a 12% polyacrylamide gel. Electrophoresis was carried out in a modular mini-Protean II electrophoresis system (Bio-Rad). Protein was then transferred to a Millipore Immobilon-P membrane by using a Bio-Rad mini-trans-blot electrophoretic transfer cell. Equal transfer efficiency was confirmed by Coomassie blue staining. Anti-p38 MAPK antibody was purchased from Cell Signaling (cat# 9212). Bovine serum albumin was used as a negative control and was not recognized by any of the antibodies tested.

In Situ Hybridization

In situ hybridizations were performed by following standard procedures. Digoxigenin-labeled antisense probes were generated from mouse cDNA clones that were kindly provided by several laboratories: *Fgf4*, Y. Chen; *Msx2*, R. Maxson; *p21*, I. Thesleff; and *Shh*, A. McMahon.

SUPPLEMENTAL DATA

Supplemental Data include two figures that show that *K14-Cre;Smad4*$^{fl/fl}$ mice do not have palate defects and that siRNA treatment alone does not interfere with palatal fusion and are available at http://www.developmentalcell.com/cgi/content/full/15/2/322/DC1/.

ACKNOWLEDGMENTS

We thank Sarah Millar for *K14-Cre* mice and thank Yiping Chen, Robert Maxson, Irma Thesleff and Andrew McMahon for plasmids. We also thank Julie Mayo for critical reading of the manuscript. This study was supported by grants from the NIDCR, NIH (DE012711 and DE014078) to Yang Chai.

Received: October 24, 2007
Revised: May 14, 2008
Accepted: June 12, 2008
Published: August 11, 2008

REFERENCES

Adachi-Yamada, T., Nakamura, M., Irie, K., Tomoyasu, Y., Sano, Y., Mori, E., Goto, S., Ueno, N., Nishida, Y., and Matsumoto, K. (1999). p38 mitogen-activated protein kinase can be involved in transforming growth factor β superfamily signal transduction in *Drosophila* wing morphogenesis. Mol. Cell. Biol. *19*, 2322–2329.

Andl, T., Ahn, K., Kairo, A., Chu, E.Y., Wine-Lee, L., Reddy, S.T., Croft, N.J., Cebra-Thomas, J.A., Metzger, D., Chambon, P., et al. (2004). Epithelial Bmpr1a regulates differentiation and proliferation in postnatal hair follicles and is essential for tooth development. Development *131*, 2257–2268.

Bei, M., Stowell, S., and Maas, R. (2004). Msx2 controls ameloblast terminal differentiation. Dev. Dyn. *231*, 758–765.

Bhowmick, N.A., Ghiassi, M., Bakin, A., Aakre, M., Lundquist, C.A., Engel, M.E., Arteaga, C.L., and Moses, H.L. (2001). Transforming growth factor-β1 mediates epithelial to mesenchymal transdifferentiation through a RhoA-dependent mechanism. Mol. Biol. Cell *12*, 27–36.

Brunet, C.L., Sharpe, P.M., and Ferguson, M.W. (1995). Inhibition of TGF-β 3 (but not TGF-β 1 or TGF-β 2) activity prevents normal mouse embryonic palate fusion. Int. J. Dev. Biol. *39*, 345–355.

Chai, Y., and Maxson, R.E., Jr. (2006). Recent advances in craniofacial morphogenesis. Dev. Dyn. *235*, 2353–2375.

Chai, Y., Jiang, X., Ito, Y., Bringas, P., Jr., Han, J., Rowitch, D.H., Soriano, P., McMahon, A.P., and Sucov, H.M. (2000). Fate of the mammalian cranial neural crest during tooth and mandibular morphogenesis. Development *127*, 1671–1679.

Cui, X.M., Warburton, D., Zhao, J., Crowe, D.L., and Shuler, C.F. (1998). Immunohistochemical localization of TGF-β type II receptor and TGF-β3 during palatogenesis in vivo and in vitro. Int. J. Dev. Biol. *42*, 817–820.

Dassule, H.R., Lewis, P., Bei, M., Maas, R., and McMahon, A. (2000). Sonic hedgehog regulates growth and morphogenesis of the tooth. Development *127*, 4775–4785.

Derynck, R., and Zhang, Y.E. (2003). Smad-dependent and Smad-independent pathways in TGF-[β] family signalling. Nature *425*, 577–584.

Dudas, M., Kim, J., Li, W.Y., Nagy, A., Larsson, J., Karlsson, S., Chai, Y., and Kaartinen, V. (2006). Epithelial and ectomesenchymal role of the type I TGF-β receptor ALK5 during facial morphogenesis and palatal fusion. Dev. Biol. *296*, 298–314.

Dumont, N., and Arteaga, C.L. (2003). Targeting the TGF β signaling network in human neoplasia. Cancer Cell *3*, 531–536.

Fitzpatrick, D.R., Denhez, F., Kondaiah, P., and Akhurst, R.J. (1990). Differential expression of TGF β isoforms in murine palatogenesis. Development *109*, 585–595.

Hartsough, M.T., and Mulder, K.M. (1995). Transforming growth factor β activation of p44mapk in proliferating cultures of epithelial cells. J. Biol. Chem. *270*, 7117–7124.

Hu, P.P., Shen, X., Huang, D., Liu, Y., Counter, C., and Wang, X.F. (1999). The MEK pathway is required for a stimulation of p21 (WAF1/CIP1) by transforming growth factor-β. J. Biol. Chem. *274*, 35381–35387.

Ito, Y., Yeo, J.Y., Chytil, A., Han, J., Bringas, P., Jr., Nakajima, A., Shuler, C.F., Moses, H.L., and Chai, Y. (2003). Conditional inactivation of Tgfbr2 in cranial neural crest causes cleft palate and calvaria defects. Development *130*, 5269–5280.

Jernvall, J., Aberg, T., Kettunen, P., Keranen, S., and Thesleff, I. (1998). The life history of an embryonic signaling center: BMP-4 induces p21 and is associated with apoptosis in the mouse tooth enamel knot. Development *125*, 161–169.

Kaartinen, V., Voncken, J.W., Shuler, C., Warburton, D., Bu, D., Heisterkamp, N., and Groffen, J. (1995). Abnormal lung development and cleft palate in mice lacking TGF-β 3 indicates defects of epithelial-mesenchymal interaction. Nat. Genet. *11*, 415–421.

Ko, S.O., Chung, I., Xu, X., Oka, S., Zhao, H., Cho, E., Deng, C.X., and Chai, Y. (2007). Smad4 is required to regulate the fate of cranial neural crest cells. Dev. Biol. *312*, 435–447.

Liu, W., Sun, X., Braut, A., Mishina, Y., Behringer, R.R., Mina, M., and Martin, J.F. (2005). Distinct functions for Bmp signaling in lip and palate fusion in mice. Development *132*, 1453–1461.

Martinez-Alvarez, C., Tudela, C., Perez-Miguelsanz, J., O'Kane, S., Puerta, J., and Ferguson, M.W. (2000). Medial edge epithelial cell fate during palatal fusion. Dev. Biol. *220*, 343–357.

Massague, J. (1998). TGF-β signal transduction. Annu. Rev. Biochem. *67*, 753–791.

Pelton, R.W., Hogan, B.L., Miller, D.A., and Moses, H.L. (1990). Differential expression of genes encoding TGFs β 1, β 2, and β 3 during murine palate formation. Dev. Biol. *141*, 456–460.

Proetzel, G., Pawlowski, S.A., Wiles, M.V., Yin, M., Boivin, G.P., Howles, P.N., Ding, J., Ferguson, M.W., and Doetschman, T. (1995). Transforming growth factor-β 3 is required for secondary palate fusion. Nat. Genet. *11*, 409–414.

Soriano, P. (1999). Generalized lacZ expression with the ROSA26 Cre reporter strain. Nat. Genet. *21*, 70–71.

Taya, Y., O'Kane, S., and Ferguson, M.W. (1999). Pathogenesis of cleft palate in TGF-β3 knockout mice. Development *126*, 3869–3879.

Thesleff, I., and Sharpe, P. (1997). Signalling networks regulating dental development. Mech. Dev. *67*, 111–123.

Tian, F., Byfield, S.D., Parks, W.T., Stuelten, C.H., Nemani, D., Zhang, Y.E., and Roberts, A.B. (2004). Smad-binding defective mutant of transforming growth factor β type I receptor enhances tumorigenesis but suppresses metastasis of breast cancer cell lines. Cancer Res. *64*, 4523–4530.

Xu, X., Bringas, P., Jr., Soriano, P., and Chai, Y. (2005). PDGFR-α signaling is critical for tooth cusp and palate morphogenesis. Dev. Dyn. *232*, 75–84.

Xu, X., Han, J., Ito, Y., Bringas, P., Jr., Urata, M.M., and Chai, Y. (2006). Cell autonomous requirement for Tgfbr2 in the disappearance of medial edge epithelium during palatal fusion. Dev. Biol. *297*, 238–248.

Yang, X., Li, C., Herrera, P.L., and Deng, C.X. (2002). Generation of Smad4/Dpc4 conditional knockout mice. Genesis *32*, 80–81.

Yu, L., Hebert, M.C., and Zhang, Y.E. (2002). TGF-β receptor-activated p38 MAP kinase mediates Smad-independent TGF-β responses. EMBO J. *21*, 3749–3759.

Zhao, X., Zhang, Z., Song, Y., Zhang, X., Zhang, Y., Hu, Y., Fromm, S.H., and Chen, Y. (2000). Transgenically ectopic expression of Bmp4 to the Msx1 mutant dental mesenchyme restores downstream gene expression but represses Shh and Bmp2 in the enamel knot of wild type tooth germ. Mech. Dev. *99*, 29–38.